

# Bifurcation Analysis About a Mathematical Model of Somitogenesis Based on the Runge–Kutta Method

Linan Guan<sup>1</sup> · Jianwei Shen<sup>2</sup>

Published online: 9 February 2018

© Springer Science+Business Media, LLC, part of Springer Nature 2018

**Abstract** In this paper, we investigated the modified two dimensional model which can explain somite patterning in embryos. It is suitable for exploring a design space of somitogenesis and can explain aspects of somitogenesis that previous models cannot. Here, we mainly studied the non-diffusing case. We have used the Hopf bifurcation theorem, the Center manifold theorem and Runge–Kutta method in our investigation. First, we investigate its dynamical behaviors and put forward a sufficient condition for the oscillation of the small network. Then, we give the mathematical simulation based on the Runge–Kutta method. In the process of solving ordinary differential equations, the four order Runge–Kutta method has the advantages of high accuracy, convergence and stability (under certain conditions), which can change the step size and do not need to calculate higher order derivatives. Therefore, it has become the most commonly used numerical solution. At the same time, we get the sufficient condition in which the bistable state of the system exists and give the numerical simulation. Because somitogenesis occupies an important position in the process of biological development, and as a pattern process can be used to study pattern formation and many aspects of embryogenesis. So our study have a great help for embryonic development, gene expression, cell differentiation. In addition, it is beneficial to study the clone animal variation problem of spinal bone number and is of great help to the treatment and prevention of defects of human spine disease.

**Keywords** Hopf bifurcation · Bistable · Somitogenesis · Runge–Kutta method

---

✉ Jianwei Shen  
xcjwshen@gmail.com

<sup>1</sup> School of Aerospace Engineering and Applied Mechanics, Tongji University, Shanghai, China

<sup>2</sup> Institute of Applied Mathematics, Xuchang University, Xuchang, China

## 1 Introduction

Vertebrate, the animal that has the spinal column, the basic morphogenesis and cell differentiation of the early embryo can be divided into two major groups [1]. One is non-repetitive patterns that include the heart, kidneys, limbs, etc. One is the repetitive pattern, including segments, feathers, and so on. Among them, somite is the transitional structure that can represent the segmental features of vertebrates.

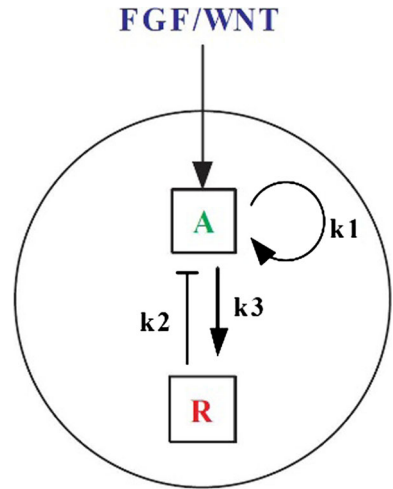
During the development of all vertebrate embryos, the presomitic mesoderm(PSM), which lies on either side of the neural tube, is progressively segmented from anterior to posterior (from approximately day 1 to day 3 in the chick embryo) into a series of transient epithelial balls called somites, which later give rise to vertebrae, muscle blocks, and skin [1, 2]. This physical budding process is prefigured by a molecular patterning process that sequentially produces stripes of gene expression along the PSM, again in an anterior-to-posterior sequence(for example *Lfng*); each stripe of expression will, in future, correspond to a subsequent somite boundary. The control of this molecular segmentation process has been a paradigmatic example of pattern formation for the last 50 years and as such has a long conceptual history of proposed underlying mechanisms [1]. Till now, many models have been proposed to explain the formation of somite, for example the clock and wavefront model, the clock and induction model, the reaction–diffusion type model, and others [3–7]. These models, though not perfect, can be used to explain the different aspects of somitogenesis [8–13]. Besides, most of these models puts forward the concept of segmentation clock. During somitogenesis in embryos, a posteriorly moving differentiation front arrests [14] the oscillations of segmentation clock genes, leaving behind a frozen, periodic pattern of expression stripes [15]. We found that mathematical theories and experimental observations used the clock wavefront model to explain the phenomenon, in which the movement of the front and the placement of the stripes in the embryo in the control of long-range molecular gradients [8, 16]. Recently, Cotterell et al. develop a new simple model which driven by short-range interactions. And they call it progressive oscillatory reaction–diffusion (PORD) system. In the model, posterior movement of the front is a local, emergent phenomenon which is not controlled by global positional information [3]. The PORD model can explain important characteristics of the formation of somite, for instance, size regulation, which can't be explained by previous reaction–diffusion models [17]. What's more, compared with the clock and wavefront model, the PORD model has some novel prediction results in FGF-inhibition and tissue cutting experiments, and they proved the correctness of their results by experiments.

Our study focuses on the non-diffusing case of the PORD model. In Sect. 2, we give the gene network represented by mathematical model firstly, then give some theoretical results. In Sect. 3, we give the numerical analysis. Finally, we summarize our results.

## 2 Experimental

Cotterell et al. [3] develop a simple model which driven by short-range interactions and it can be used to explain somite patterning in embryos. When they analyzed the dynamics and behavior of networks in the large stalactite, they found that they operate in a fundamentally different way from the clock and wavefront model. The simplest version of the mechanism is a network of only two nodes (Fig. 1), comprising a cell-autonomous

**Fig. 1** The minimal somite-patterning circuit [3] in our study, which comprises an activator molecule  $A$  (green) and a diffusible repressor  $R$  (red).  $k_1, k_2,$  and  $k_3$  are the strengths of regulatory interactions between  $A$  and  $R$ ,  $\mu$  is a fixed decay constant, and  $F$  is the regulatory input of the FGF/WNT gradient onto  $A$ .  $\beta$  is the background regulatory input of  $A$ . (Colour figure online)



activator ( $A$ ), which is itself activated by the FGF signal, and a diffusible repressor ( $R$ ), whose levels are defined by the following equations

$$\begin{aligned} \frac{\partial A}{\partial t} &= \frac{k_1 A + k_2 R + F + \beta}{1 + k_1 A + k_2 R + F + \beta} - \mu A \\ \frac{\partial R}{\partial t} &= \frac{k_3 A}{1 + k_3 A} - \mu R \end{aligned} \tag{1}$$

where  $k_1, k_2,$  and  $k_3$  define the strengths of regulatory interactions between  $A$  and  $R$ ,  $\mu$  is a fixed decay constant, and  $F$  is the regulatory input of the FGF/WNT gradient onto  $A$ .  $\beta$  is the background regulatory input of  $A$ (the gene receiving the morphogen activation).

### 2.1 Hopf Bifurcation

Suppose Eq. (1) has a fixed point  $(A, R) = (A_0, R_0)$ , which may depend on the parameter  $k_1$ , let  $x(t) = A(t) - A_0, y(t) = R(t) - R_0$ . Then the linearized system of Eq. (1) at origin is as follows

$$\begin{aligned} \frac{\partial x}{\partial t} &= m_{11}x + m_{12}y \\ \frac{\partial y}{\partial t} &= m_{21}x + m_{22}y \end{aligned} \tag{2}$$

where

$$\begin{aligned} m_{11} &= \frac{k_1}{(1 + k_1 A_0 + k_2 R_0 + F + \beta)^2} - \mu, \\ m_{12} &= \frac{k_2}{(1 + k_1 A_0 + k_2 R_0 + F + \beta)^2}, \\ m_{21} &= \frac{k_3}{(1 + k_3 A_0)^2}, m_{22} = -\mu. \end{aligned}$$

Defining the  $D(\lambda)$  as follows

$$D(\lambda) = \begin{pmatrix} m_{11} & m_{12} \\ m_{21} & m_{22} \end{pmatrix} \tag{3}$$

then we can get the characteristic equation from (3)

$$\det(\lambda I - D(\lambda)) = 0 \tag{4}$$

where  $I$  is the  $2 \times 2$  identity matrix, and the characteristic Eq. (4) has the following form

$$\lambda^2 - Tr\lambda + \delta = 0 \tag{5}$$

where  $Tr = m_{11} + m_{22}$ ,  $\delta = m_{11}m_{22} - m_{12}m_{21}$ , and when  $Tr^2 - 4\delta < 0$ , we have  $\lambda_{1,2} = \frac{Tr \pm i\sqrt{4\delta - Tr^2}}{2}$ .

Then, the following theoretical results can be obtained:

**Theorem 1** *The Hopf bifurcation occurs in the 2-dimensional system which should satisfy the following conditions here.*

- (i)  $Tr = m_{11} + m_{22} = 0$ ,
- (ii)  $\delta = m_{11}m_{22} - m_{12}m_{21} > 0$ ,
- (iii)  $d = \frac{\partial Tr(k_1)}{\partial k_1} \Big|_{k_1=k_1^0} \neq 0$ .

(When  $k_1 = k_1^0$ , Eqs. (1) have a fixed point  $(A_0, R_0)$ ) Let  $a = \frac{1}{16}(f_{uuu} + f_{uvv} + g_{uuv} + g_{vvv}) + \frac{1}{16\omega}(f_{uv}(f_{uu} + f_{vv}) - g_{uv}(g_{uu} + g_{vv}) - f_{uu}g_{uu} + f_{vv}g_{vv})$  (see appendix for the calculation method [23]), We can get another theoretical results.

**Theorem 2** *Let  $a$  and  $d$  be defined as above,*

- (i) *There is a supercritical (subcritical) Hopf bifurcation if  $a < 0$  ( $a > 0$ ),*
- (ii) *An unique curve of periodic solutions bifurcates from point  $(A_0, R_0)$  into the region  $k_1 > k_1^0$  if  $ad < 0$  or  $k_1 < k_1^0$  if  $ad > 0$ . The point  $(A_0, R_0)$  is a stable fixed point for  $k_1 > k_1^0$  (resp.  $k_1 < k_1^0$ ) and an unstable fixed point for  $k_1 < k_1^0$  (resp.  $k_1 > k_1^0$ ) if  $d < 0$  (resp.  $d > 0$ ). Meanwhile, if the periodic solutions exist, there will be an unstable (resp. stable) periodic solution when the point  $(A_0, R_0)$  is stable (resp. unstable).*

By using Hopf bifurcation theory, our theorem 1, 2 can be proved. The proof process can be found in [18, 19]. Therefore, we omit the process of proving the theorem 1,2 here. In the next part, we use a numerical example to illustrate the correctness of our theoretical results.

**Lemma 1** *When,  $Tr = 0$ , that is*

$$k_1 = \frac{1 - 4\mu A_0(1 + k_2 R_0 + F + \beta) \pm \sqrt{(4\mu A_0(1 + k_2 R_0 + F + \beta) - 1)^2 - 16\mu^2 A_0^2(1 + k_2 R_0 + F + \beta)^2}}{4\mu A_0^2},$$

and  $\delta < 0$ , then there is a Neutral saddle at  $(A_0, R_0)$ .

Neutral saddle without bifurcate significance and has nothing to do with stable diversity. So we don't do too much research about it.

### 2.2 Bistable State Analysis

First we set both equations of (1) equal to zero, and solved the second equation for  $R$

$$R = \frac{k_3x}{\mu(1 + k_3x)} \tag{7}$$

and then substituted it into the first equation of (1). This gave us the following equation for the fixed points of the system.

$$k_1k_3\mu x^3 + (k_1\mu + k_2k_3 + (1 + F + \beta)\mu k_3 - k_1k_3)x^2 + ((1 + F + \beta)\mu - k_1 - k_2k_3/\mu - (F + \beta)k_3)x - (F + \beta) = 0 \tag{7}$$

Let

$$a = k_1k_3\mu, b = k_1\mu + k_2k_3 + (1 + F + \beta)\mu k_3 - k_1k_3, \\ c = (1 + F + \beta)\mu - k_1 - k_2k_3/\mu - (F + \beta)k_3, d = -(F + \beta).$$

We get the equation as follows:

$$h(x) = ax^3 + bx^2 + cx + d = 0 \tag{8}$$

The discriminant of the derivative of  $h(x)$  is

$$\Delta = 4b^2 - 12ac \tag{9}$$

We define the discriminant of  $h(x)$  as follows

$$\Delta' = (b^2 - 4ac)(c^2 - 4bd) - ad(27ad - 2bc) \tag{10}$$

Then, we can get the following theoretical results:

#### Theorem 3

- (i) When  $\Delta > 0$  or  $\Delta \leq 0$  and  $\Delta' < 0, h(x)$  have only one real root;
- (ii) When  $\Delta > 0$  and  $\Delta' = 0, h(x)$  have two different real roots;
- (iii) When  $\Delta > 0$  and  $\Delta' > 0, h(x)$  have three different real roots. And at this time, the system have a bistable state.

In the third part, we demonstrate the above theoretical results applied the Runge–Kutta method by a numerical example.

## 3 Results

### 3.1 Hopf Bifurcation and Limite Cycle

Without loss of generality, if we take  $k_1^0 = 0.103572, k_2 = -2.28, k_3 = 0.099, \mu = 0.05, F = 1, \beta = 0.5$ , the Eqs. (1) becomes

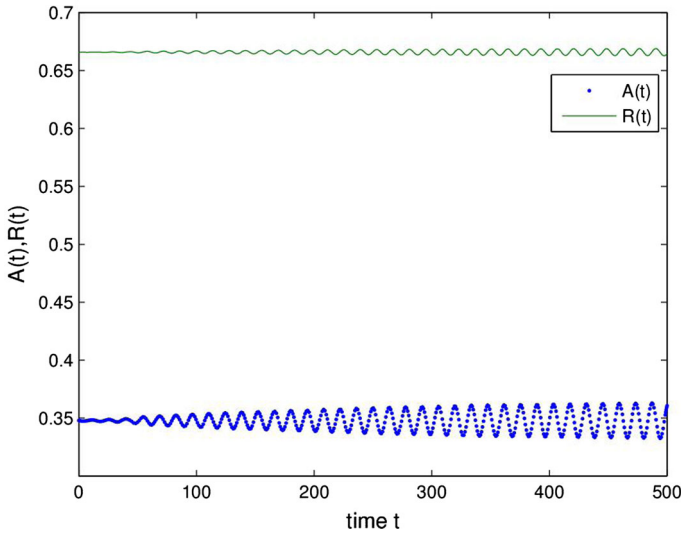


**Fig. 2** A periodic solution bifurcated from equilibrium  $(A_0, R_0)$

$$\begin{aligned} \frac{\partial A}{\partial t} &= \frac{0.103572A - 2.28R + 1.5}{1 + 0.103572A - 2.28R + 1.5} - 0.05A \\ \frac{\partial R}{\partial t} &= \frac{0.099A}{1 + 0.099A} - 0.05R \end{aligned} \tag{6}$$

Such a system has a positive equilibrium  $(A_0, R_0) = (0.347915, 0.665934)$ . By using the Theorem 1 and Theorem 2 we can obtain that  $d \approx 0.448568, a \approx 0.015599$ , so there is a subcritical Hopf bifurcation. Thus, for value of the  $k_1^0$ , the Theorem 1 applies. When  $k_1^0 \approx 0.103572$ , there is a Hopf bifurcation (see Fig. 2). We have  $d > 0$  and. Hence the point  $(A_0, R_0)$  is an unstable fixed point for  $k_1 > 0.103572$  and a stable fixed point for  $k_1 < 0.103572$ , whilst there is a unstable limit cycle for  $k_1 < 0.103572$  (see Figs. 3, 4).

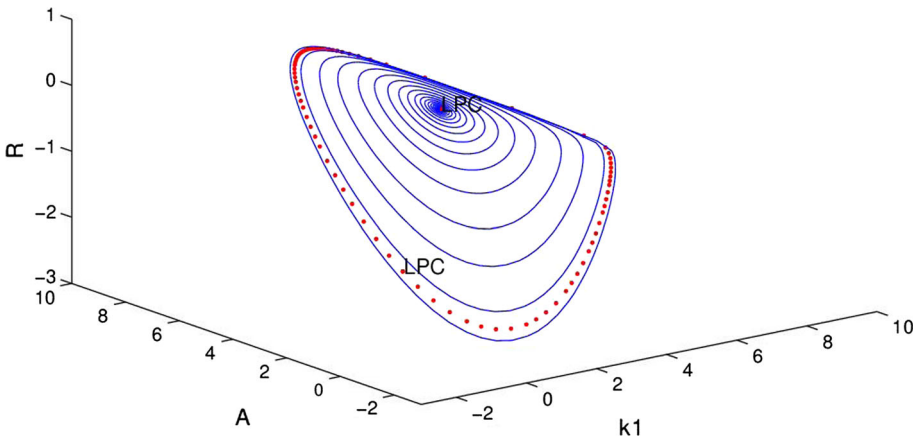


**Fig. 3** An unstable limit cycle from equilibrium  $(A_0, R_0)$ . Software used is the MATCONT package [20] in MATLAB (The Math-Works, Inc., Natick, Massachusetts, USA)

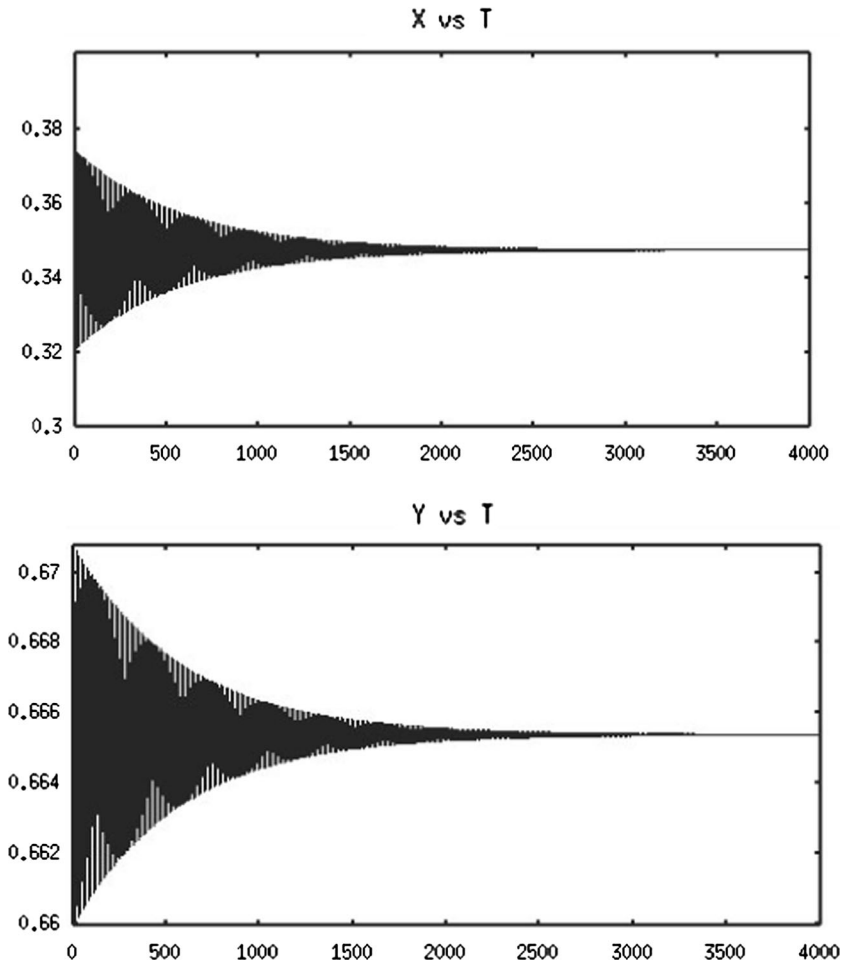


**Fig. 4** The time series of Eqs. (1).  $X$  and  $Y$  represent the concentration of activator  $A$  and repressor  $R$ , respectively. It's before the Hopf bifurcation at the parameter value  $k_1 = 0.1$  with initial point  $(A_0, R_0) = (0.347915, 0.665934)$ , which is inside the limit cycle, the origin is stable and the limit cycle is unstable, the orbit spirals to the origin

### 3.2 Bistable

Let us now fix the parameter value  $k_1 = 0.103572$ ,  $k_2 = -2.28$ ,  $k_3 = 0.099$ ,  $\mu = 0.05$ ,  $F = 1$ ,  $\beta = 0.5$ ,  $A_0 = 0.347915$ ,  $R_0 = 0.665934$ , then  $\Delta = 0.163837617$ ,  $\Delta' = 0.03903007478$ , the Theorem 2 applies, we know the system have a bistable state (see Fig. 5).

## 4 Conclusion

In this paper, we used a simple two-dimensional model to analyze the dynamics and behavior of networks in the large stalactite. Particularly, we mainly studied dynamical behaviors of the two-dimensional model by using the Runge–Kutta method, at the

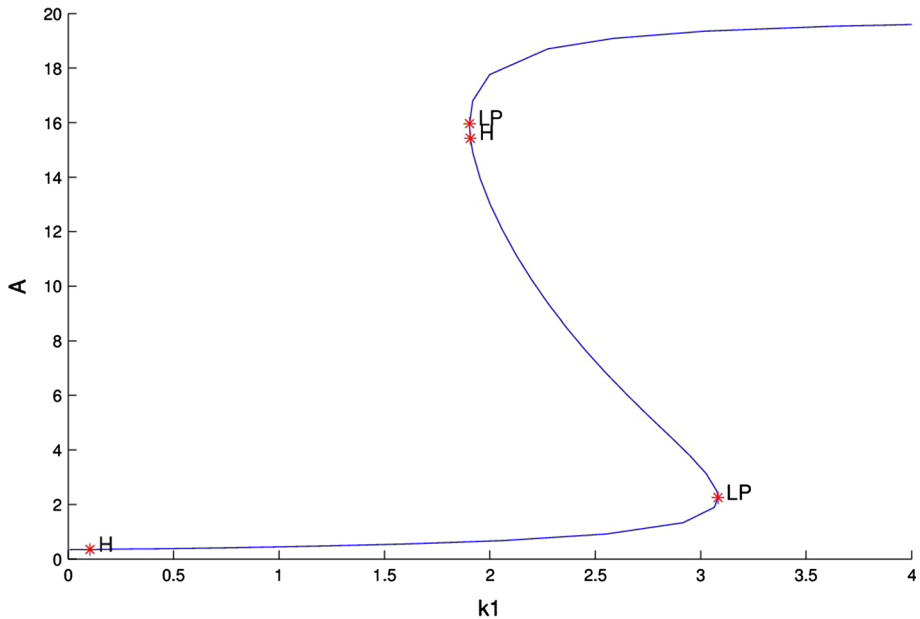


**Fig. 5** A branch of equilibria in the  $(k_1, A(t))$ -plane displaying bistable

meantime, we derived the sufficient conditions of oscillation by taking advantage of Hopf bifurcation theory [21–23]. Specifically, we came to an conclusion that there is a periodic solutions when parameter  $k_1$  reach its critical value and it is a subcritical Hopf bifurcation for which marks the instability of limit cycles destroyed in Hopf bifurcation. In addition, we also got the conditions of the system to produce bistable state, and numerical examples are given. Based on the above theoretical results, we can have a better understanding of somitogenesis in embryos.

By studying the two-dimensional model, we know that oscillation depends on the parameter by utilizing single parameter bifurcation analysis. we take the strength as the bifurcation parameter, and found that the oscillation depends on the parameter. A numerical example is given by using the Runge–Kutta method. Moreover, we obtained the condition for producing bistability of the system. Recent biological experiment [24–28] evinced that somitogenesis in the process of biological development occupies an important position and as a pattern process can be used to study pattern formation and many aspects of embryogenesis. So our study have a great help for embryonic development, gene expression, cell differentiation. In addition, it is beneficial to study the clone animal variation problem of spinal bone number and is of great help to the treatment and prevention of defects of human spine disease. In the present study, we merely use a simplified model to explore the dynamical behavior of somitogenesis. In the future, we will investigate the effects of delay, noise and diffusion on somitogenesis.

**Acknowledgements** This work is supported by National Natural Science Foundation of China (No. 11772291, 11572278), Innovation Scientists and Technicians Troop Construction Projects of Henan Province (No. 2017JR0013).



## Compliance with ethical standards

**Conflict of Interest** The authors declare that the research was conducted in the absence of any commercial or financial relationships that could be construed as a potential conflict of interest.

## References

- Cooke, J. (1975). Control of somite number during morphogenesis of a vertebrate, *Xenopus laevis*[J]. *Nature*, 254(5479), 196–199.
- McGrew, M. J., & Pourquie, O. (1998). Somitogenesis: Segmenting a vertebrate. *Current Opinion in Genetics & Development*, 8(4), 487–493.
- Cotterell, J., Robert-Moreno, A., & Sharpe, J. (2015). A local, self-organizing reaction-diffusion model can explain somite patterning in embryos. *Cell Systems*, 1(4), 257–269.
- Kulesa, P. M., Schnell, S., Rudloff, S., Baker, R. E., & Maini, P. K. (2007). From segment to somite: Segmentation to epithelialization analyzed within quantitative frameworks. *Developmental Dynamics*, 236, 1392–1402.
- Cooke, J., & Zeeman, E. C. (1976). A clock and wavefront model for control of the number of repeated structures during animal morphogenesis. *Journal of Theoretical Biology*, 58, 455–476.
- Meinhardt, H. (1996). Model of biological pattern formation: Common mechanism in plant and animal development. *International Journal of Developmental Biology*, 40, 123–134.
- Polezhaev, A. A. (1992). A mathematical model of the mechanism of vertebrate somitic segmentation. *Journal of Theoretical Biology*, 156(2), 169–181.
- Schnell, S., & Maini, P. K. (2000). Clock and induction model for somitogenesis. *Developmental Dynamics*, 217(4), 415–420.
- Collier, J. R., Mcinerney, D., Schnell, S., Maini, P. K., Gavaghan, D. J., Houston, P., et al. (2000). A cell cycle model for somitogenesis: Mathematical formulation and numerical simulation. *Journal of Theoretical Biology*, 207(3), 305–316.
- Kerszberg, M., & Wolpert, L. (2000). A clock and trail model for somite formation, specialization and polarization. *Journal of Theoretical Biology*, 205(3), 505–510.
- Herrgen, L., Ares, S., Morelli, L. G., Schroter, C., Julicher, F., & Oates, A. C. (2010). Intercellular coupling regulates the period of the segmentation clock. *Current Biology*, 20, 1244–1253.
- Baker, R. E., Schnell, S., & Maini, P. K. (2006). A mathematical investigation of a clock and wavefront model for somitogenesis. *Journal of Mathematical Biology*, 52, 458–482.
- Baker, R. E., Schnell, S., & Maini, P. K. (2006). A clock and wavefront mechanism for somite formation. *Development Biology*, 293, 116–126.
- Polezhaev, A. A. (1995). Mathematical modelling of the mechanism of vertebrate somitic segmentation. *Journal of Biological Systems*, 3(04), 1041–1051.
- Lin, G., & Slack, J. M. (2008). Requirement for Wnt and FGF signaling in *Xenopus* tadpole tail regeneration. *Development Biology*, 316, 323–335.
- Polezhaev, A. A. (1995). Mathematical model of segmentation in somitogenesis in vertebrates. *Biophysics*, 3(40), 583–589.
- Murray, P. J., Maini, P. K., & Baker, R. E. (2011). The clock and wavefront model revisited. *Journal of Theoretical Biology*, 283, 227–238.
- Munoz Alicea, R. (2011). Introduction to bifurcations and the Hopf bifurcation theorem for planar systems. *Operation for Mathematics*, 640, 11.
- Kuznetsov, Y. (2006). Andronov-Hopf bifurcation. *Scholarpedia*, 1(10), 1858.
- Dhooge, A., Govaerts, W., & Kuznetsov, Y. A. (2003). MATCONT: A Matlab package for numerical bifurcation analysis of ODEs. *ACM Transactions on Mathematical Software*, 29, 141–164.
- Kuehn, C. (2012). From first lyapunov coefficients to maximal canards. *International Journal of Bifurcation and Chaos*, 20(5), 1467–1475.
- Sarmah, H. K., Baishya, T. K., & Das, M. C. (2014). Hopf-bifurcation in a two dimensional nonlinear differential equation. *International Journal of Modern Engineering and Research Technology*, 4, 2249–6645.
- Das D., Banerjee, D. & Bhattacharjee, J. K. (2013). Super-critical and Sub-Critical Hopf bifurcations in two and three dimensions. [arXiv:1309.5470v1](https://arxiv.org/abs/1309.5470v1).
- Chen, K. W., Liao, K. L., & Shih, C. W. (2018). The kinetics in mathematical models on segmentation clock genes in zebrafish. *Journal of Mathematical Biology*, 76(1–2), 97–150.

25. Shimono, Y., Yamaguchi, I., Ishimatsu, K., Akao, A., Ogawa, Y., Jimbo, Y., & Kotani, K. (2018). Evaluation of heuristic reductions of a model for the segmentation clock in zebrafish. In *IEEJ transactions on electrical and electronic engineering*.
26. Ajima, R., Suzuki, E., & Saga, Y. (2017). Pofut1 point-mutations that disrupt O-fucosyltransferase activity destabilize the protein and abolish Notch1 signaling during mouse somitogenesis. *PLoS ONE*, *12*(11), e0187248.
27. Gallagher, T. L., Tietz, K. T., Morrow, Z. T., McCammon, J. M., Goldrich, M. L., Derr, N. L., et al. (2017). Pnrc2 regulates 3'UTR-mediated decay of segmentation clock-associated transcripts during zebrafish segmentation. *Developmental Biology*, *429*(1), 225–239.
28. Uriu, K., Bhavna, R., Oates, A. C., & Morelli, L. G. (2017). A framework for quantification and physical modeling of cell mixing applied to oscillator synchronization in vertebrate somitogenesis. *Biology Open*, *6*, 1235.



**Linan Guan** was born in March 1991, she got the bachelor's degree at Pingdingshan University in 2014, Master's degree at Zhengzhou University in 2017. Now she is studying for a doctorate at Tongji University. Her research direction is modeling, analysis and control of nonlinear systems.



**Jianwei Shen** received his M.S. degree from Kunming University of Science and Technology, Yunnan, China, in 2003, and Ph.D. degree at Northwestern Polytechnical University, Shanxi, in 2006, China. Since 2012, he has been a professor of Xuchang University. His research is algorithm of complex system and dynamical mechanism.